

Article

# Ultrasonic Treatment Induced Fluoride Conversion Coating without Pores for High Corrosion Resistance of Mg Alloy

Sheng Li, Laihua Yi \*, Xiongxiang Zhu and Tongfang Liu

College of Automotive Engineering, Hunan Mechanical & Electrical Polytechnic, Changsha 410151, China; S11021060@163.com (S.L.); Ylh090306@163.com (X.Z.); nancy1210@163.com (T.L.)

\* Correspondence: 173701007@csu.edu.cn

Received: 9 September 2020; Accepted: 12 October 2020; Published: 19 October 2020



**Abstract:** Fluoride conversion ( $\text{MgF}_2$ ) coating with facile preparation and good adhesion is promising to protect Mg alloy, but defects of pores in the coating lead to limited corrosion resistance. In this study, a compact and dense  $\text{MgF}_2$  coating was prepared by the combination of fluoride treatment and ultrasonic treatment. The ultrasonically treated  $\text{MgF}_2$  coating showed a compact and dense structure without pores at the frequency of 28 kHz. The chemical compositions of the coating were mainly composed of F and Mg elements. The corrosion potential of the ultrasonically treated Mg alloy shifted towards the noble direction in the electrochemical tests. The corrosion current density decreased due to the protectiveness of  $\text{MgF}_2$  coating without defects of pores or cracks. During immersion tests for 24 h, the ultrasonically treated Mg alloy exhibited the lowest  $\text{H}_2$  evolution ( $0.32 \text{ mL/cm}^2$ ) and pH value (7.3), which confirmed the enhanced anti-corrosion ability of  $\text{MgF}_2$  coating. Hence, the ultrasonically treated fluoride coating had great potentials for their use in anti-corrosion applications of Mg alloy.

**Keywords:** corrosion resistance; fluoride conversion coating; Mg alloy; ultrasonic treatment

## 1. Introduction

As one of the lightweight metals with low density and high mechanical properties, Mg alloy has attracted significant interest in the automotive and aviation industry. However, the lightweight applications of Mg alloy have been hindered due to the highly corrosive tendency [1–3]. Mg alloy is extremely sensitive to galvanic corrosion, leading to a rapid corrosion [3–5]. In addition, Mg alloy also has a tendency of localized corrosion, leading to a quick failure of mechanical properties [6,7]. To protect Mg alloy against corrosion and to maintain their mechanical integrity, various kinds of anti-corrosion techniques have been developed, such as phosphating treatment, microarc oxidation and polymer coating [8–12]. Although these surface modifications are ways of preventing corrosion and maintaining the mechanical strength of Mg alloy to some extent [13], there are a lack of chemical bonding interfaces between Mg alloy substrate and the protective coating.

Fluoride treatment seems to be an effective way to prepare a protective chemical fluoride conversion coating ( $\text{MgF}_2$ ) for high Mg alloy corrosion resistance recently. Dvorsky et al. [14] found that fluoride treatment could reduce the corrosion rate of WE43 Mg alloy by half due to good chemical adhesion on the substrate. Panemangalore et al. [15] developed a uniform fluoride conversion coating using fluoride treatment, which improved corrosion resistance of Mg–3Zn–0.5Er alloy. It should be noted that hydrogen ( $\text{H}_2$ ) is produced during fluoride treatment, leading to a porous coating. Moreover, the fluoride conversion coating is usually thin [16–18]. Consequently, the anti-corrosion property is often inferior, as well as the thickness of the coating. It is generally thought that fluoride treatment can be mainly used as a pre-treatment process. Hence, more researches are needed to prepare reliable fluoride conversion coating with desirable protective characteristics.

Ultrasonic treatment is reported to tailor the microstructure of the solution-metal interface with the spread of ultrasound wave through liquid media, which brings about physical, mechanical changes of coatings [19,20]. Studies show that ultrasonic in the phosphating process produced high corrosion resistance coating with fewer pores [21]. Yang et al. [22] investigated the effect of ultrasonic on the microstructure of manganese phosphating coating and found that ultrasonic induced a uniform fine-grained coating with low porosity. Domnikov et al. [23] found that ultrasonic in the phosphating process could generate less porous coating, thereby greatly improving corrosion resistance. Qu et al. [24] found that the corrosion resistance of ultrasonic micro-arc oxidation was better than that of micro-arc oxidation coating on Mg alloy. Hence, the application of the ultrasonic treatment may be valuable to prepare compact  $\text{MgF}_2$  coating without obvious defects of pores or cracks. To our best knowledge, few papers reported the ultrasonically treated  $\text{MgF}_2$  coating on Mg alloy. This study aimed to explore fluoride conversion coating on Mg alloy via ultrasonic treatment to improve its corrosion resistance. To obtain a better understanding, the mechanisms of ultrasonically treated fluoride conversion layer, compositions, thickness, and porosity, etc., were investigated. The protectiveness of fluoride conversion coating on Mg alloy in a corrosive environment was discussed.

## 2. Materials and Methods

### 2.1. Experimental Materials

The AZ31 alloy is one of the most popular Mg alloys with aluminum. Due to its good mechanical properties and magnificent strength to weight ratio, the material offers great potentials for the aviation and automotive industry. Thus, substrate material was AZ31 Mg alloy (0.004 Mn, 2.98 Al, 0.007 Fe, 0.97 Zn, 0.005 Ni, 0.05 Ca, 0.02 Si, and Mg Bal. wt.%). The AZ31 Mg alloy sheets (20 mm  $\times$  10 mm  $\times$  5 mm in size) were ground using different SiC papers and polished on diamond paste. Finally, the polished Mg alloy was washed in ethanol for the removal of residues. Hydrofluoric acid (HF, 38 wt.%, Shandong Xuchen Chemical Technology Co., Ltd., Zibo, China) was used to generate fluoride conversion coating on the Mg alloy substrate.

### 2.2. Fluoride Conversion Coating Preparation

The fluoride conversion ( $\text{MgF}_2$ ) coating was produced via dipping of the polished Mg alloy substrate into HF for 14 h in a sealed plastic beaker (15 cm  $\times$  10 cm  $\times$  8 cm). The different frequencies of 0 (untreated, F-treatment), 14 and 28 kHz under ultrasonic treatment (U-treatment) were chosen for the processing of the  $\text{MgF}_2$  coatings on Mg alloy substrate. Mg alloy samples were subsequently removed from the container and dried in hot air from a thermal dryer (HS-101-0, Wuhan Hans Instrument Equipment Co., Ltd., Wuhan, China) for 2 h after the set treatment time. The schematic illustration of ultrasonically treated fluoride coating on Mg alloy was exhibited in Figure 1.

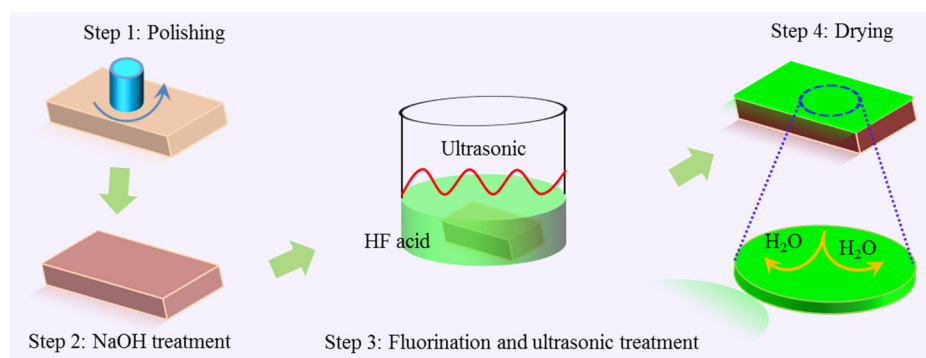


**Figure 1.** Schematic illustration showing the preparation process of ultrasonically treated fluoride coating on Mg alloy.

### 2.3. Characterization

The cross-sectional and surface morphologies of MgF<sub>2</sub> coating were studied by scanning electron microscopy (SEM, XL-30FEG, Eindhoven, The Netherlands) at an accelerating voltage of 15 kV), which was equipped by an energy dispersive spectroscopy (EDS, Oxford, Eindhoven, The Netherlands) attachment. EDS was used to analyze the element compositions of the fluoride conversion layer. The microstructure of the layer was also investigated by SEM. The layer thickness of the samples was determined according to SEM images in the cross-sections. Pores and cracks were evaluated using image analysis (Image J) of surface morphologies.

### 2.4. Electrochemical Properties

The corrosion resistance of the ultrasonically treated fluoride coating Mg alloy was investigated using electrochemical tests [25,26]. A three-electrode system with a saturated calomel reference electrode and a platinum counter electrode was used to carry out electrochemical tests at 25 °C. The ultrasonically treated fluoride coating Mg alloy acted as the working electrode. The tests were performed in NaCl aqueous solution with a pH of 7 at room temperature using an electrochemical workstation (Zahner, Kronach, Germany). The exposure area of the working electrode to NaCl aqueous solution was 1 cm<sup>2</sup>. The potentiodynamic polarization curves were obtained from −2.1 to −0.8 V at the rate of 15 mV/s. The corrosion potentials and corrosion current density were determined via Tafel extrapolation based on potentiodynamic polarization curves. The electrochemical impedance spectroscopy (EIS) tests were conducted at a disturbance frequency ranging from 10<sup>−2</sup> to 10<sup>5</sup> Hz under a perturbation signal-amplitude of 15 mV.

### 2.5. Statistical Analysis

The test values were expressed by the mean values ± standard deviation and analyzed by the *t*-test. A *p*-value of less than 0.05 was considered significant statistically.

## 3. Results and Discussion

Surface morphologies of ultrasonically treated fluoride coating Mg alloy at the frequency of 0, 14 and 28 kHz are shown in Figure 2, respectively. Obviously, there were differences in surface microstructure. The surface of HF-treated Mg alloy (0 kHz) was covered with many pores and cracks in Figure 2a,d. The high amount of pores and cracks could bring about a fast penetration of corrosive medium through the MgF<sub>2</sub> coating to Mg alloy substrate, leading to the corrosion attack of the coated samples. After ultrasonic treatment at 14 kHz, MgF<sub>2</sub> coating in Figure 2b,e was smoother and fewer pores and cracks were found. Moreover, the surface of the MgF<sub>2</sub> coating in Figure 2c,f after ultrasonic treatment at 28 kHz exhibited a compact structure without obvious pores and cracks. Such a compact MgF<sub>2</sub> coating acted as a good barrier against the ingress of corrosive medium, which was responsible for the durability of the protective layer. The pores mainly came from H<sub>2</sub>, which was generated in the displacement reaction between HF and Mg. Ultrasonic treatment at 28 kHz induced strong physical and chemical changes at the interface of the solution-metal through ultrasound wave. On the one hand, due to the ultrasound wave H<sub>2</sub> bubbles might smoothly flow, hence greatly reducing defects caused by the residual gas; on the other hand, the ultrasound wave greatly enhanced local pressure in the liquid, which brought about the collapse of H<sub>2</sub> bubbles. Moreover, it was reported that ultrasonic treatment could tailor the microstructure of the solution–metal interface with the spread of ultrasound wave through liquid media due to ultrasonic cavitation [19,20]. In this way, ultrasonic treatment might increase not only the nucleation rate but also the nucleation number of MgF<sub>2</sub> grains, thereby producing fluoride conversion coating with better coverage and seal of pores and cracks. Hence, proper ultrasonic treatment facilitated uniform and compact coating deposit with fine microstructure. In contrast, without ultrasonic treatment witnessed more pores due to the residual gas, as shown in Figure 2g.

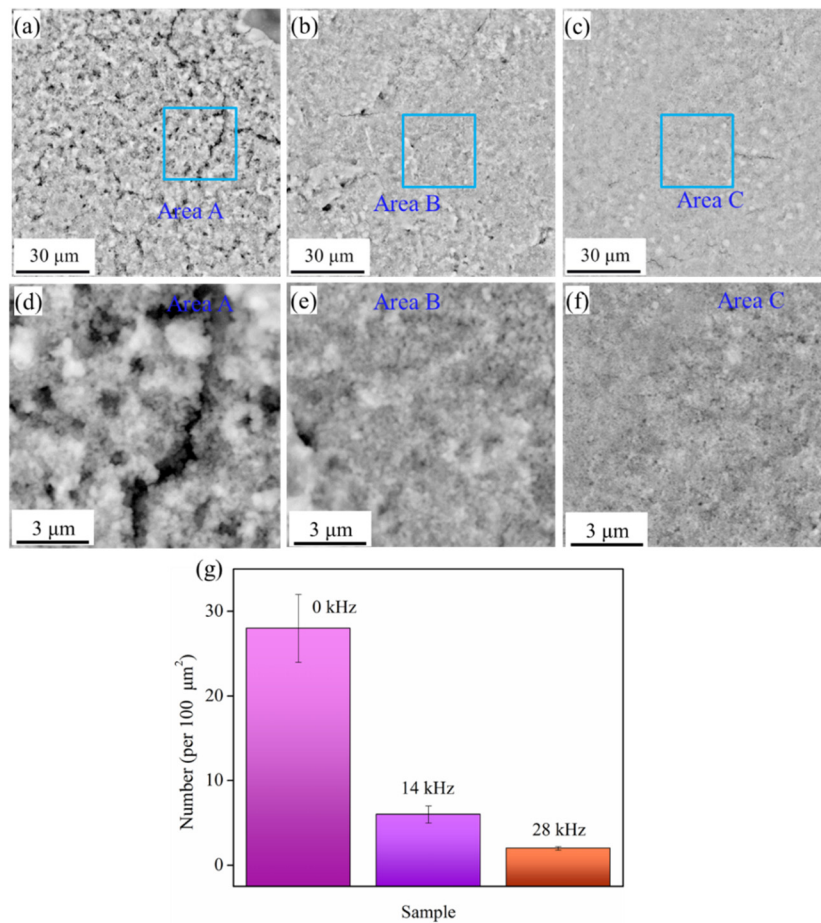


**Figure 2.** Morphologies of Mg alloy surfaces of ultrasonically treated fluoride coating at the frequency of (a) 0, (b) 14 and (c) 28 kHz, respectively, (d–f) enlarged images of area A, B, C, respectively, and (g) the number of pores per 100 μm<sup>2</sup>.

The surface chemical elements of U-treatment Mg alloy were further examined by EDS in this study and it was shown in Figure 3. It could be observed that the distributions of F and Mg elements were indicated in red and blue, respectively, which demonstrated that the MgF<sub>2</sub> coating was uniformly distributed on Mg alloy substrate in Figure 3. The following reaction of Equations (1) and (2) between Mg and HF was thought to take place on Mg alloy substrate during ultrasonic treatment in HF solution:



The in-situ reactions produced MgF<sub>2</sub> layers on Mg alloy substrate. Owing to the nature barrier of the MgF<sub>2</sub> coating [27,28], the corrosion reaction decreased after immersion in NaCl solution. However, in those chemical reactions, H<sub>2</sub> was produced. It would remain within the MgF<sub>2</sub> coating or escape from the coating along cracks, which would only offer a limited increase in Mg alloy corrosion resistance. Porous MgF<sub>2</sub> coating could not act as an effective barrier from the perpetration of corrosive medium and thereby corrosion would proceed along these defects in the MgF<sub>2</sub> coating, significantly reducing the corrosion resistance of the protective layer.

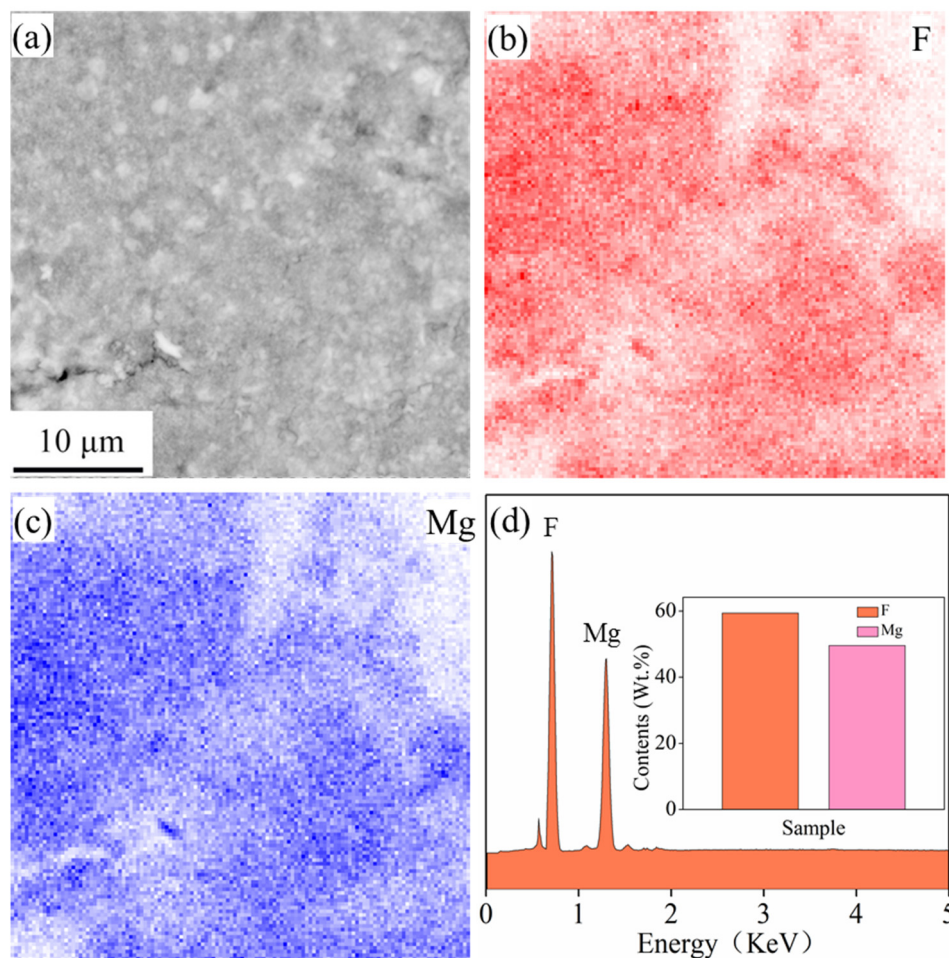


**Figure 3.** The energy dispersive (EDS) map analysis of the surface of U-treatment Mg alloy at the frequency of 28 kHz: (a) SEM surface, (b) F distribution, (c) Mg distribution, and (d) Contents of F and Mg elements.

Cross-section of Mg alloy surfaces with EDS analysis of ultrasonically treated fluoride coating at 0, 14 and 28 kHz are shown in Figure 4a–d, respectively. It could be seen that the thickness of the  $\text{MgF}_2$  coating was about 18, 21 and 28 μm in Figure 4e, which demonstrated that all the Mg alloy substrate was mainly covered with the  $\text{MgF}_2$  coating. Although  $\text{MgF}_2$  coating formed on Mg alloy substrate, small defects, such as pores and cracks, could be found in the coating and the interface between the coating and the substrate, as exhibited in Figure 4a. These pores formed because of the evolution of  $\text{H}_2$  during the coating procedure. Corrosion would proceed along these pores and cracks, breaking the protective  $\text{MgF}_2$  layer. To protect Mg alloy from corrosion in corrosive conditions, ultrasonic treatment was proposed to eliminate the pores or cracks. As shown in Figure 4b,c, the cross-section of U-treatment samples presented much more compact and dense morphologies. It should be noted that no pores or cracks were visible in the cross-section of the U-treatment sample at 28 kHz, indicating that ultrasonic treatment well covered micro-pores and -cracks in the  $\text{MgF}_2$  layer. Moreover, the interface in Figure 4c was tightly bonded onto Mg alloy substrate, suggesting a good binding force. The enlarged view of area A in Figure 4f showed that no serious defects, including pores or cracks that induced fracture and peeling of the coating, could be observed. This suggested the  $\text{MgF}_2$  coating was well adhered to the Mg alloy substrate chemically and it was expected to have a strong adhesive and protective ability, which represented the coating's ability to impede corrosion to some extent. The cross-section analyses revealed that ultrasonic treatment effectively removed the pores and cracks, and promoted the formation of  $\text{MgF}_2$  coating with a compact and dense microstructure. This study provided a new way of eliminating defects produced by the  $\text{H}_2$  in the coating.

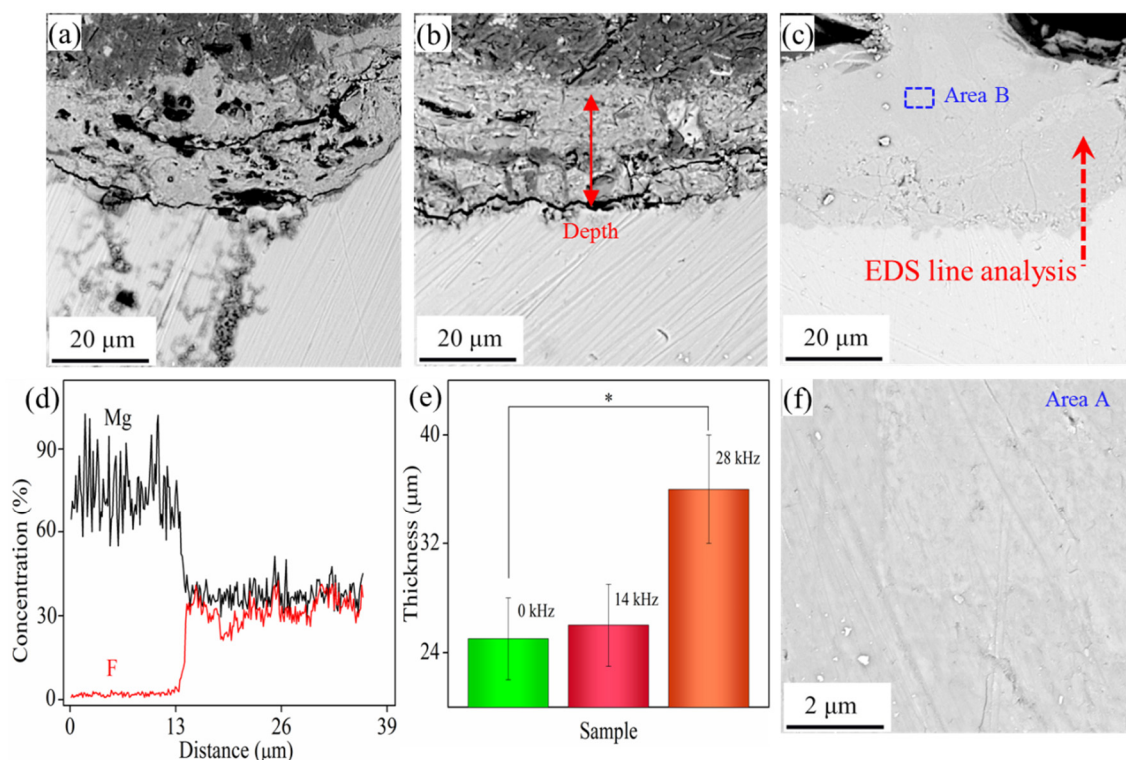


**Figure 4.** Cross-sections of Mg alloy surfaces of ultrasonically treated fluoride coating at (a) 0, (b) 14 and (c) 28 kHz, respectively; (d) compositions along an EDS scan line, (e) Average thickness of the  $\text{MgF}_2$  layer on Mg alloy and (f) enlarged images of area A of the cross-section of Mg alloy surface.

To determine the influences of ultrasonic treatment on the electrochemical corrosion characteristics of the  $\text{MgF}_2$  coated Mg alloy, electrochemical tests were performed via a three-electrode system, as shown in Figure 5a. The obtained corrosion potential and corrosion current density are exhibited in Figure 5b,c, respectively. It could be found that the  $\text{MgF}_2$  coating on Mg alloy substrate brought about the increase of corrosion resistance from both corrosion potential and corrosion current density point of view. This was due to coating isolation, which was basically consistent in agreement with the reports in the literature [29,30]. It should be noted that differences were found between U-treatment and F-treatment samples. The corrosion potential of the U-treatment sample was more positive compared to that of the F-treatment sample. Moreover, the U-treatment sample exhibited a decrease in corrosion current density. These results showed that the use of ultrasonic treatment was an effective way of improving corrosion resistance of the  $\text{MgF}_2$  coated Mg alloy.

EIS tests are non-destructive techniques in which the frequency change in impedance could be instantaneously measured in response to an alternating current voltage. Information in relation to anti-corrosion properties could be obtained based on the tests. Hence, EIS was a useful and valuable tool to reveal the protection ability of coatings to the underlying Mg alloy substrate. Nyquist plots of ultrasonically treated fluoride coating are shown in Figure 6a. After ultrasonic treatment at 14 kHz,  $\text{MgF}_2$  coating exhibited an increase in the diameter of the semi-circle over the untreated (0 kHz), which was representative of larger charge transfer resistance at the interface of electrolyte and samples. After ultrasonic treatment at 28 kHz,  $\text{MgF}_2$  coating further increased the charge transfer resistance, as observed by the largest diameter of the semi-circle. Impedance magnitude of Bode plots is exhibited in Figure 6b. It was clearly observed at a low frequency range ( $1\text{--}10^{-2}$  Hz) that  $\text{MgF}_2$  coating with ultrasonic treatment at 28 kHz showed the highest impedance magnitude ( $3568\text{ ohm}\cdot\text{cm}^2$ ). The phase angle of Bode plots in Figure 6c also exhibited obvious differences among as-prepared samples at a high frequency range ( $10^5\text{--}10$  Hz). The results of both Bode and Nyquist plots proved that ultrasonically treated fluoride coating had better corrosion protection effects.

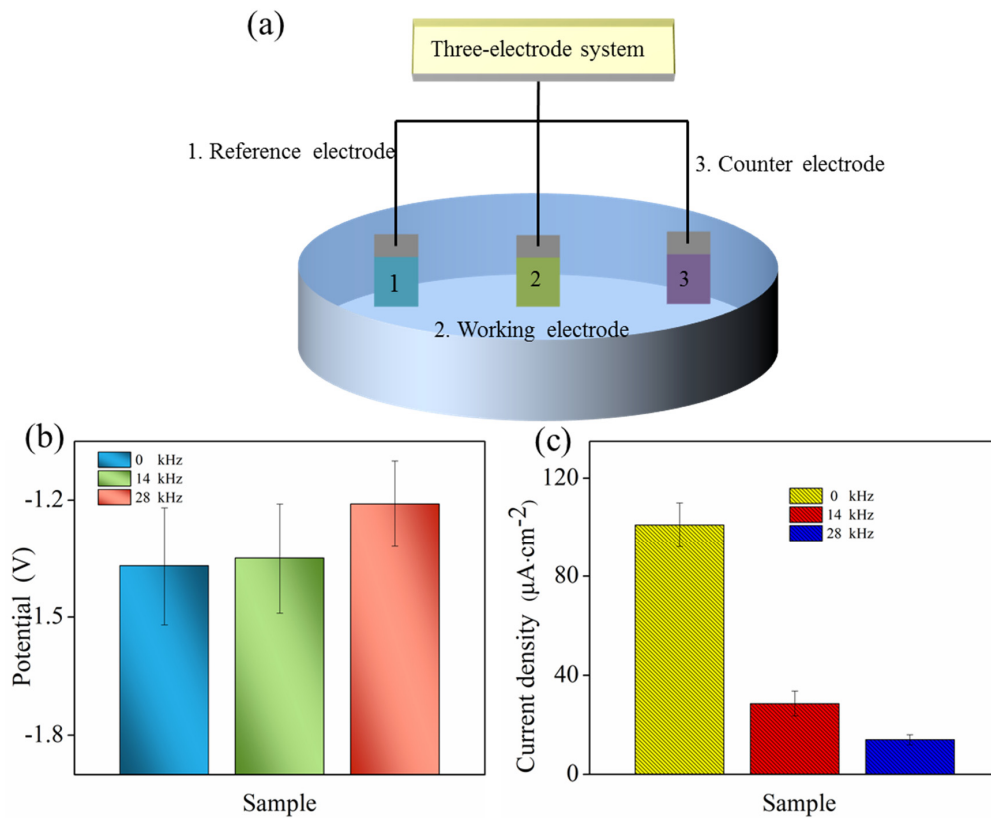


**Figure 5.** Electrochemical corrosion characteristics of U-treatment Mg alloy with F-treatment Mg alloy as the control group: (a) explanation of the measurement method; (b) corrosion potential and (c) corrosion current density.

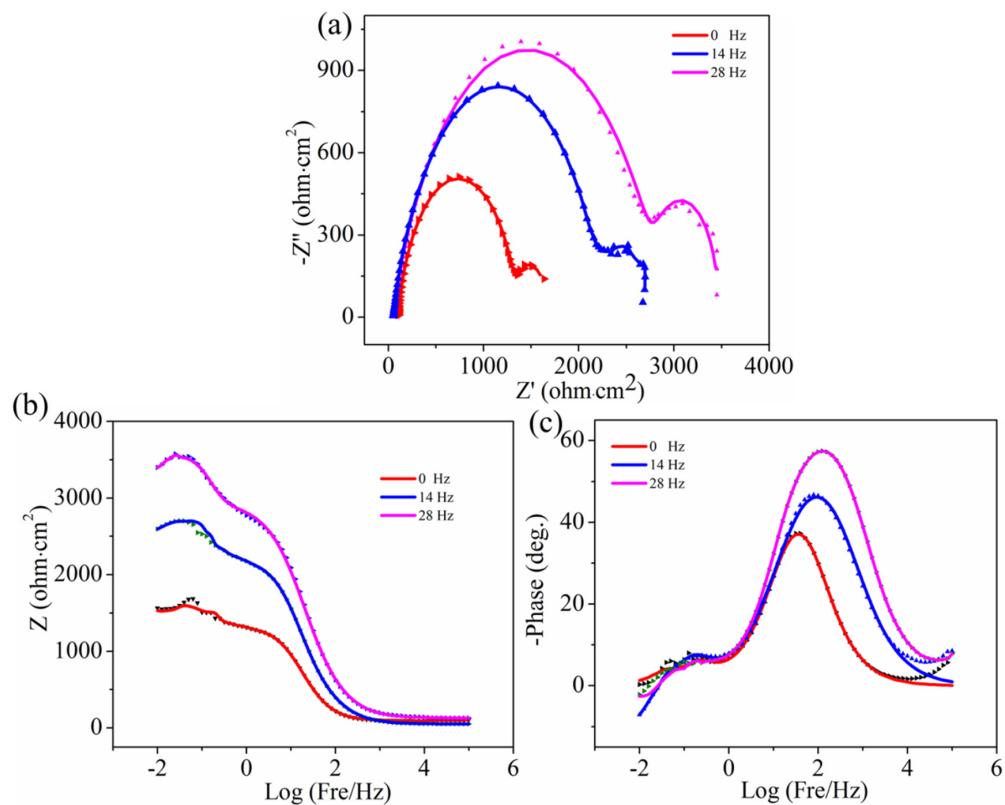


**Figure 6.** Anti-corrosive properties of ultrasonically treated fluoride coating via EIS tests: (a) Nyquist plots, (b) impedance magnitude and (c) phase angle of Bode plots.

The protectiveness of the  $\text{MgF}_2$  coating was further evaluated by means of  $\text{H}_2$  evolution and pH variation.  $\text{H}_2$  from corrosion reactions was measured to evaluate the anti-corrosion property in the tests, as shown in Figure 7a. The samples were immersed in a 3.5% NaCl solution for 24 h and  $\text{H}_2$  was collected during the tests. It was found that the  $\text{H}_2$  bubble soon evolved for the F-treatment sample at the beginning. This was due to the fact that the corrosive medium penetrated through the top  $\text{MgF}_2$  coating layer to Mg alloy substrate, and the corrosion of the Mg alloy started. Some  $\text{H}_2$  bubbles were observed for the U-treatment sample at the frequency of 14 kHz at the early stage of the immersion tests. In the case of the U-treatment sample at the frequency of 28 kHz, the  $\text{H}_2$  bubble was obviously inhibited. After a long period of immersion time, only several bubbles were found. The U-treatment Mg alloy at the frequency of 28 kHz exhibited the lowest  $\text{H}_2$  evolution ( $0.32 \text{ mL/cm}^2$ ) during immersion tests for 24 h, as shown in Figure 7b. These findings of ultrasonically treated fluoride coating Mg alloy were attributed to its slow corrosion rate. The above results showed that the ultrasonic procedure was an important reason for the improved corrosion resistance. Furthermore, the pH of the solution after immersion in the 3.5% NaCl solution for 24 h was measured and exhibited in Figure 7c. It could be found that U-treatment samples possessed low pH values (7.3), which also confirmed that ultrasonic treatment significantly enhanced the anti-corrosion ability of  $\text{MgF}_2$  coating.

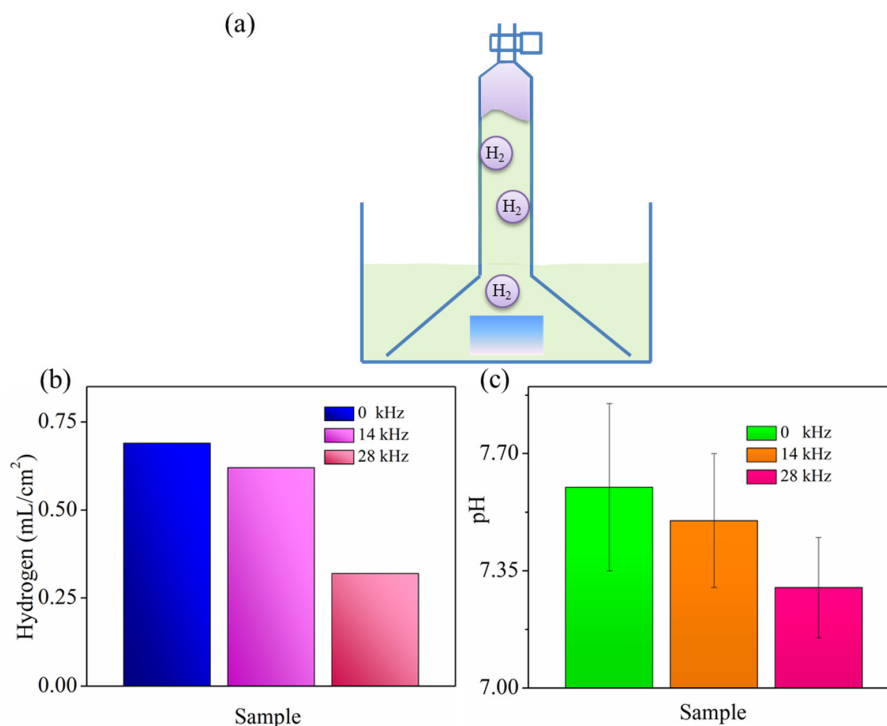


**Figure 7.** Immersion test results in a 3.5% NaCl solution for 24 h: (a) schematic diagram of immersion test, (b) hydrogen evolution and (c) pH changes of solution.

Mg alloy corrosion resistance could be improved by U-treatment, in which the sample was dipped into HF solution under ultrasonic treatment. The surface of the sample was covered by a  $\text{MgF}_2$  layer with a dense and compact microstructure, which acted as a barrier and prevented corrosion reactions between Mg alloy substrate and corrosive medium. This agreed with the electrochemical test results, suggesting that the corrosion resistance of Mg alloy was obviously improved via ultrasonic treatment.

To reduce the corrosion of Mg alloy, the role played by the ultrasonically treated fluoride coating could be explained by considering the corrosion process of Mg alloy in a corrosive environment, as shown in Figure 8. Mg alloy was reactive and easily corroded in aqueous medium due to the reaction between  $\text{H}_2\text{O}$  and Mg. In this study, due to the reaction between Mg and HF,  $\text{MgF}_2$  coating was produced. However, considering defects, mainly pores and cracks shown in Figure 8a in the

coating, this self-protecting coating was unstable and it resulted in the penetration of corrosive medium, which rapidly corroded the Mg alloy substrate. It has been reported that the protectiveness of  $\text{MgF}_2$  layers only held for a short time. For example, Conceição et al. found that after 20 h of exposure in corrosion medium, the impedance of Mg alloy coated with  $\text{MgF}_2$  layer decreased by four decades [31]. This suggested that the corrosive medium penetrated through the coating, arriving at Mg alloy substrate over short time periods. The short-term protectiveness it provided was related to pores and cracks in the  $\text{MgF}_2$  coating, which resulted in corrosion of Mg alloy underneath the coating, producing undermining effects, as evidenced in tests. Hence, to improve the long-term protectiveness, the coating defects, such as pores and cracks, should be suppressed via the coating process optimization. In this study, a controlled defect behavior could be established by ultrasonically treated fluoride coating on Mg alloy substrate with optimum frequency. Firstly, ultrasound waves might make  $\text{H}_2$  bubbles flow smoothly, which significantly reduced the number of residual  $\text{H}_2$  bubbles, as shown in Figure 8b. Secondly, ultrasonic treatment transferred energy among solutions, the interface of the solution-metal and  $\text{MgF}_2$  layers through ultrasound wave. The local pressure around an  $\text{H}_2$  bubble was enhanced and simultaneously the temperature increased, which facilitated the collapse of the  $\text{H}_2$  bubble. It should be noted that ultrasonic cavitation, which was a common phenomenon during ultrasonic treatment in liquid conditions, might also facilitate the formation of  $\text{MgF}_2$  coating with compact microstructure. The ultrasonic cavitation contained bubble formation, growth and implosion at the solution–metal interfacial [19,32], as shown in Figure 8c, which could not only accelerate the fresh HF solution to diffuse towards the reaction interface but also increase the nucleation rate and number of  $\text{MgF}_2$  grains. This would seal the cracks or pores in the  $\text{MgF}_2$  layer, producing better coverage among grains. In this way, a dense and compact  $\text{MgF}_2$  coating with high protectiveness formed on Mg alloy substrate, as exhibited in Figure 8d. The preliminary studies showed promising results of the ultrasonic treatment in eliminating the defects of pores or cracks in the  $\text{MgF}_2$  coating.

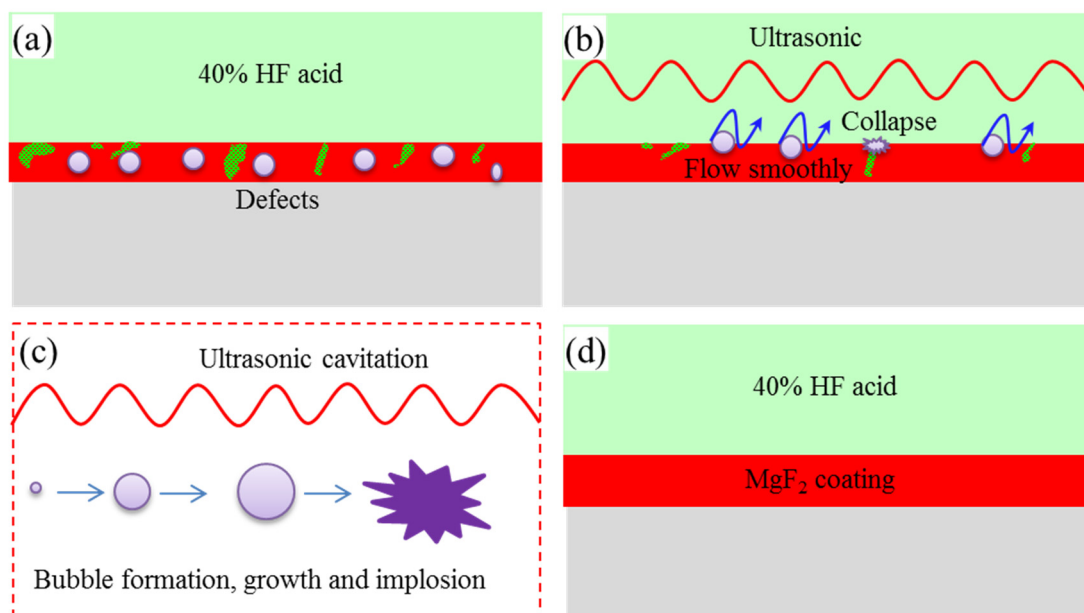


**Figure 8.** Schematic illustration of the protectiveness of F-treatment and U-treatment Mg alloys: (a) the F-treatment Mg alloy, (b) the U-treatment Mg alloy, (c) effects of ultrasonic cavitation during ultrasonic treatment in liquid conditions, and (d) the ultrasonically treated fluoride coating without defects of pores or cracks.

AZ31 Mg alloy with magnificent strength to weight ratio is emerging as an alternative in car body replacements like in luggage retainers and car panels. Highly reactive nature of Mg resulted in surface oxidation with atmospheric  $\text{H}_2\text{O}$  or  $\text{O}_2$ , immediately after it extruded from a twin roll casting

machinery. Moreover, exposure of AZ31 Mg alloy to the environment during storage or handling among the operation steps may lead to an electrochemically driven corrosion. Improving corrosion resistance to avoid this early corrosion is therefore essential [10,33,34]. For the purpose, the processing methods need to possess temporary anti-corrosive protective ability to protect the semi-finished AZ31 Mg alloy. Therefore, the ultrasonically treated fluoride coating without defects was introduced for temporary protection of AZ31 Mg alloy against corrosion in this study. In addition, the ultrasonically treated fluoride coating may have been potentially applied in temporary implants, such as a urinary stent, vascular stent, and bone fixators. MgF<sub>2</sub> coating can not only increase new mineral deposition, but also provide a layer against too rapid biodegradation [35–37].

#### 4. Conclusions

The protective coating of an MgF<sub>2</sub> layer with solid interfacial bonding and no obvious defects was prepared by the combination of fluoride treatment and ultrasonic treatment, which effectively enhanced corrosion resistance. The effect of ultrasonic treatment was investigated and discussed in detail. The main findings of this study were as follows:

- (1) A dense and compact MgF<sub>2</sub> coating was successfully prepared by the combination of fluoride treatment and ultrasonic treatment. When the frequency was 28 kHz during ultrasonic treatment, the surface microstructure was uniform. The chemical compositions were mainly composed of F and Mg elements.
- (2) Electrochemical tests in NaCl solution exhibited improved corrosion resistance. The corrosion potential of U-treatment Mg alloy constantly shifted towards the noble direction. The corrosion current density decreased due to the protectiveness of MgF<sub>2</sub> coating without pores or cracks.
- (3) Immersion tests showed an improvement in the short-term instability of the MgF<sub>2</sub> coating after ultrasonic treatment, which provided enough corrosion protection, inhibiting not only pH increase but also gas cavities formation. The improvement in corrosion resistance that MgF<sub>2</sub> coating induced on Mg alloy was due to the formation of a compact structure without defects. This reduced the channel of the corrosive medium into the Mg alloy surface and thereby strengthened coating passivation ability. Consequently, it could be concluded that ultrasonically treated fluoride coating had much promise for their use in anti-corrosion applications of Mg alloy, such as automotive, aviation industry and temporary implants.

**Author Contributions:** S.L. writing and preparation of the original draft; L.Y. writing and review; X.Z. discussion and editing; T.L. revision and formal analysis. All authors have read and agreed to the published version of the manuscript.

**Funding:** The work was financially supported by a project supported by the Scientific Research Fund of the Hunan Provincial Education Department (Nos. 18C1387, 19C0664).

**Acknowledgments:** The authors wished to thank Hunan Mechanical and Electrical Polytechnic.

**Conflicts of Interest:** The authors declare no conflict of interest.

#### References

1. Xiang, D.; Li, S.; Yi, L.-H.; Liu, T.-F.; Liu, J.; Yang, C.-M.; Zhou, L.-H. In Situ Formation of intermetallic compound bonding by laser cladding Al<sub>2</sub>O<sub>3</sub> to enhance the corrosion resistance of AZ<sub>31</sub> magnesium alloy. *Lasers Eng.* **2020**, *45*, 127.
2. Li, S.; Yi, L.; Liu, T.; Ji, B.; Yang, C.; Zhou, L. Al<sub>2</sub>O<sub>3</sub> eliminating defects in the Al coating by laser cladding to improve corrosion and wear resistance of Mg alloy. *Mater. Corros.* **2020**, *71*, 980. [[CrossRef](#)]
3. Li, S.; Yi, L.; Liu, T.; Deng, H.; Ji, B.; Zhang, K.; Zhou, L. Formation of a protective layer against corrosion on Mg alloy via alkali pretreatment followed by vanillic acid treatment. *Mater. Corros.* **2020**, *21*, 991. [[CrossRef](#)]
4. Rahmati, M.; Raeissi, K.; Toroghinejad, M.R.; Hakimizad, A.; Santamaria, M. Effect of pulse current mode on microstructure, composition and corrosion performance of the coatings produced by plasma electrolytic oxidation on AZ31 Mg alloy. *Coatings* **2019**, *9*, 688. [[CrossRef](#)]

5. Xie, J.; Zhang, J.; Liu, S.; Li, Z.; Zhang, L.; Wu, R.; Hou, L.; Zhang, M. Hydrothermal synthesis of protective coating on Mg alloy for degradable implant applications. *Coatings* **2019**, *9*, 160. [[CrossRef](#)]
6. Mehrjou, B.; Dehghan-Baniani, D.; Shi, M.; Shanaghi, A.; Wang, G.; Liu, L.; Qasim, A.M.; Chu, P.K. Nanopatterned silk-coated AZ<sub>31</sub> magnesium alloy with enhanced antibacterial and corrosion properties. *Mater. Sci. Eng. C* **2020**, *18*, 111173. [[CrossRef](#)]
7. Vaughan, M.; Karayan, A.; Srivastava, A.; Mansoor, B.; Seitz, J.; Eifler, R.; Karaman, I.; Castaneda, H.; Maier, H. The effects of severe plastic deformation on the mechanical and corrosion characteristics of a bioresorbable Mg-ZKQX6000 alloy. *Mater. Sci. Eng. C* **2020**, *21*, 111130. [[CrossRef](#)]
8. Pezzato, L.; Babbolin, R.; Cerchier, P.; Marigo, M.; Dolcet, P.; Dabalà, M.; Brunelli, K. Sealing of PEO coated AZ<sub>91</sub> magnesium alloy using solutions containing neodymium. *Corros. Sci.* **2020**, *13*, 108741. [[CrossRef](#)]
9. Wei, X.; Liu, P.; Ma, S.; Li, Z.; Peng, X.; Deng, R.; Zhao, Q. Improvement on corrosion resistance and biocompatibility of ZK60 magnesium alloy by carboxyl ion implantation. *Corros. Sci.* **2020**, *44*, 108729. [[CrossRef](#)]
10. Korrapati, V.K.; Scharnagl, N.; Letzig, D.; Zheludkevich, M.L. Self-assembled layers for the temporary corrosion protection of magnesium-AZ<sub>31</sub> alloy. *Corros. Sci.* **2020**, *27*, 108619. [[CrossRef](#)]
11. Toorani, M.; Aliofkhaei, M.; Mahdavian, M.; Naderi, R. Effective PEO/Silane pretreatment of epoxy coating applied on AZ<sub>31</sub>B Mg alloy for corrosion protection. *Corros. Sci.* **2020**, *11*, 108608. [[CrossRef](#)]
12. Buzolin, R.H.; Volovitch, P.; Maltseva, A.; Lamaka, S.; Blawert, C.; Mendis, C.L.; Lohmüller, A.; Kainer, K.U.; Hort, N. Thixomolded AZ91D and MRI153M magnesium alloys and their enhanced corrosion resistance. *Mater. Corros.* **2020**, *71*, 339–351. [[CrossRef](#)]
13. Xue, Y.; Pang, X.; Jiang, B.; Jahed, H.; Wang, D. Characterization of the corrosion performances of as-cast Mg–Al and Mg–Zn magnesium alloys with microarc oxidation coatings. *Mater. Corros.* **2020**, *71*, 992–1006. [[CrossRef](#)]
14. Dvorsky, D.; Kubasek, J.; Vojtech, D. Corrosion protection of WE43 magnesium alloy by fluoride conversion coating. *Manuf. Technol.* **2017**, *17*, 440–446. [[CrossRef](#)]
15. Panemangalore, D.B.; Shabadi, R.; Gupta, M.; Ji, G. Effect of fluoride coatings on the corrosion behavior of Mg–Zn–Er alloys. *Surf. Interfaces* **2019**, *14*, 72–81. [[CrossRef](#)]
16. Chiu, K.; Wong, M.; Cheng, F.; Man, H. Characterization and corrosion studies of fluoride conversion coating on degradable Mg implants. *Surf. Coat. Technol.* **2007**, *202*, 590–598. [[CrossRef](#)]
17. Yan, T.; Tan, L.; Zhang, B.; Yang, K. Fluoride conversion coating on biodegradable AZ<sub>31</sub>B magnesium alloy. *J. Mater. Sci. Technol.* **2014**, *30*, 666–674. [[CrossRef](#)]
18. Saranya, K.; Kalaiyaran, M.; Chatterjee, S.; Rajendran, N. Dynamic electrochemical impedance study of fluoride conversion coating on AZ<sub>31</sub> magnesium alloy to improve bio-adaptability for orthopedic application. *Mater. Corros.* **2019**, *70*, 698–710. [[CrossRef](#)]
19. Ma, F-F.; Zhang, D.; Huang, T.; Zhang, N.; Wang, Y. Ultrasonication-assisted deposition of graphene oxide on electrospun poly (vinylidene fluoride) membrane and the adsorption behavior. *Chem. Eng. J.* **2019**, *358*, 1065–1073. [[CrossRef](#)]
20. Zhan, Y.; Wu, J.; Xia, H.; Yan, N.; Fei, G.; Yuan, G. Dispersion and exfoliation of graphene in rubber by an ultrasonically-assisted latex mixing and in situ reduction process. *Macromol. Mater. Eng.* **2011**, *296*, 590–602. [[CrossRef](#)]
21. Sun, X.; Liu, M.; Song, J.; Xu, Y. Corrosion behaviors of hybrid ultrasonic phosphating coatings on carbon steel in simulated 150 °C hot-dry-rock fluids. *Geothermics* **2020**, *86*, 101807. [[CrossRef](#)]
22. Yang, J.; Kim, J.; Chun, J.S. A study of the effect of ultrasonics on manganese phosphating of steel. *Thin Solid Films* **1983**, *101*, 193–200. [[CrossRef](#)]
23. Domnikov, L. The effect of ultrasonics on the phosphating process. *Metal Finish.* **1967**, *65*, 55–57.
24. Qu, L.; Li, M.; Liu, M.; Zhang, E.; Ma, C. Microstructure and corrosion resistance of ultrasonic micro-arc oxidation biocoatings on magnesium alloy. *J. Adv. Ceram.* **2013**, *2*, 227–234. [[CrossRef](#)]
25. Saha, A.; Mondal, A.; Maiti, S.; Ghosh, S.C.; Mahanty, S.; Panda, A.B. A facile method for the synthesis of a C@MoO<sub>2</sub> hollow yolk–shell structure and its electrochemical properties as a faradaic electrode. *Mater. Chem. Front.* **2017**, *1*, 1585–1593. [[CrossRef](#)]
26. Pérez, E.; Carretero, N.; Sandoval, S.; Fuertes, A.; Tobias, G.; Casañ-Pastor, N. Nitro-graphene oxide in iridium oxide hybrids: Electrochemical modulation of N-graphene redox states and charge capacities. *Mater. Chem. Front.* **2020**, *4*, 1421–1433. [[CrossRef](#)]

27. Ren, M.; Cai, S.; Liu, T.; Huang, K.; Wang, X.; Zhao, H.; Niu, S.; Zhang, R.; Wu, X. Calcium phosphate glass/MgF<sub>2</sub> double layered composite coating for improving the corrosion resistance of magnesium alloy. *J. Alloy. Compd.* **2014**, *591*, 34–40. [[CrossRef](#)]
28. Riaz, U.; Rahman, Z.U.; Asgar, H.; Shah, U.; Shabib, I.; Haider, W. An insight into the effect of buffer layer on the electrochemical performance of MgF<sub>2</sub> coated magnesium alloy ZK60. *Surf. Coat. Technol.* **2018**, *344*, 514–521. [[CrossRef](#)]
29. Zang, D.; Zhu, R.; Zhang, W.; Yu, X.; Lin, L.; Guo, X.; Liu, M.; Jiang, L. Corrosion-resistant superhydrophobic coatings on Mg alloy surfaces inspired by Lotus seedpod. *Adv. Funct. Mater.* **2017**, *27*, 1605446. [[CrossRef](#)]
30. Ho, C.-Y.; Huang, S.-M.; Lee, S.-T.; Chang, Y.-J. Evaluation of synthesized graphene oxide as corrosion protection film coating on steel substrate by electrophoretic deposition. *Appl. Surf. Sci.* **2019**, *477*, 226–231. [[CrossRef](#)]
31. Da Conceicao, T.F.; Scharnagl, N.; Blawert, C.; Dietzel, W.; Kainer, K. Surface modification of magnesium alloy AZ<sub>31</sub> by hydrofluoric acid treatment and its effect on the corrosion behavior. *Thin Solid Films* **2010**, *518*, 5209–5218. [[CrossRef](#)]
32. Zou, Y.; Zhang, Z.; Liu, S.; Chen, D.; Wang, G.; Wang, Y.; Zhang, M.; Chen, Y. Ultrasonic-assisted electroless Ni-P plating on dual phase Mg-Li alloy. *J. Electrochem. Soc.* **2014**, *162*, C64. [[CrossRef](#)]
33. Ismail, N.; Hussain, Z.; Abdalla, K. Effect of strontium pretreatment on magnesium alloy evaluated by immersion test. *AIP Conf. Proc.* **2020**, 2267. [[CrossRef](#)]
34. Toorani, M.; Aliofkhaeaei, M. Review of electrochemical properties of hybrid coating systems on Mg with plasma electrolytic oxidation process as pretreatment. *Surf. Interfaces* **2019**, *14*, 262–295. [[CrossRef](#)]
35. Kamrani, S.; Fleck, C. Biodegradable magnesium alloys as temporary orthopaedic implants: A review. *BioMetals* **2019**, *32*, 185–193. [[CrossRef](#)]
36. Dilshad, T.; Rahim, S.A.; Hanas, T. Polyvinyl alcohol/magnesium phosphate composite coated Mg–Ca Alloy for biodegradable orthopaedic implant applications. *Mater. Res. Express* **2019**, *6*, 1165–1167.
37. Dubey, A.; Jaiswal, S.; Haldar, S.; Roy, P.; Lahiri, D. Functionally gradient magnesium based composite for temporary orthopedic implant with improved corrosion resistance and osteogenic properties. *Biomed. Mater.* **2020**. [[CrossRef](#)]

**Publisher’s Note:** MDPI stays neutral with regard to jurisdictional claims in published maps and institutional affiliations.



© 2020 by the authors. Licensee MDPI, Basel, Switzerland. This article is an open access article distributed under the terms and conditions of the Creative Commons Attribution (CC BY) license (<http://creativecommons.org/licenses/by/4.0/>).